Extracellular K^+ and Ba^{2+} mediate voltage-dependent inactivation of the outward-rectifying K^+ channel encoded by the yeast gene *TOK1*

Paola Vergani[a], Thomas Miosga[b], Simon M. Jarvis[c], Michael R. Blatt[a,*]

[a] *Laboratory of Plant Physiology and Biophysics, Wye College, University of London, Wye, Kent TN25 5AH, UK*
[b] *Institut für Mikrobiologie und Genetik, Technische Hochschule Darmstadt, Schnittspahnstrasse 10, D-64287 Darmstadt, Germany*
[c] *Research School of Biosciences, University of Kent, Canterbury, Kent CT2 7NJ, UK*

Received 14 January 1997

Abstract **Gating of the yeast K^+ channel encoded by the *Saccharomyces cerevisiae* gene TOK1, unlike other outward-rectifying K^+ channels that have been cloned, is promoted by membrane voltage (inside positive-going) and repressed by extracellular K^+. When expressed in *Xenopus laevis* oocytes, the TOK1p current rectified strongly outward, its activation shifting in parallel with the K^+ equilibrium potential when the external K^+ concentration ($[K^+]_o$) was increased above 3 mM. Analysis of the TOK1p current indicated that two kinetic components contributed to the conductance and the voltage sensitivity of the conductance. By contrast, the $[K^+]_o$ sensitivity of the current was accommodated entirely within the slow-relaxing component; it was diminished near 1 mM $[K^+]_o$, and at submillimolar concentrations the voltage dependence of the TOK1p conductance was insensitive to $[K^+]_o$. External Rb^+, the K^+ channel blockers Cs^+ and Ba^{2+} – but not Na^+, Ca^{2+} or Mg^{2+} – substituted for K^+ in control of TOK1p activation, indicating a specificity in cation interaction with the TOK1p gate. These and additional results indicate that external K^+ acts as a ligand to inactivate the TOK1p channel, and they implicate a gating process mediated by a single cation binding site within the membrane electric field, but distinct from the permeation pathway.**

Key words: Voltage-dependent inactivation; Outward-rectifying K^+ channel; Extracellular ion; *Saccharomyces cerevisiae*

1. Introduction

A number of outward-rectifying K^+ channels have now been identified in plants and fungi that differ from the archetypal outward rectifiers of animal cells. Delayed and A-type K^+ channels of animals are commonly activated on membrane depolarisation over a relatively narrow voltage range – exhibiting an apparent gating charge near four – and this voltage sensitivity is largely independent of extracellular K^+ concentration [1,4,5]. The pore-forming subunits of these K^+ channels all belong to a super-family of proteins that share a highly conserved structural motif of six putative membrane-spanning domains (S1–S6) that include a transmembrane voltage 'sensor' (S4) and a loop (H5 or P) between domains S5 and S6 that comprises much of the lining of the aqueous pore [4–6].

By contrast, the outward-rectifying K^+ channels that predominate in many higher-plant cells [7–9] show a comparatively weak dependence on membrane voltage. Furthermore, these channels also exhibit a pronounced sensitivity to the extracellular K^+ concentration ($[K^+]_o$): the voltage dependence for gating of these channels is displaced roughly in parallel with the equilibrium potential for K^+ (E_K). The structural elements giving rise to this $[K^+]_o$ dependence are unknown, but the gating characteristics are shared by TOK1p (= YKC1 = YORK = DUK1 [2,3,10,11]), which constitutes the major outward-rectifying K^+ channel of *Saccharomyces cerevisiae* [11] and was recently shown to be encoded by open reading frame *J0911* on chromosome X [12]. Intriguing features of the predicted TOK1p sequence are the apparent absence of an S4-like voltage sensor and a second P-loop domain which may contribute to properties of the channel pore, ion selectivity and block, or it may act as a sensor for $[K^+]_o$, or both. We have examined TOK1p expressed in *Xenopus* oocytes to characterise the action of K^+ and other extracellular cations on gating of the current. The results indicate that K^+, like Cs^+ and Ba^{2+}, acts as a ligand to effect voltage-dependent inactivation or block of the TOK1p K^+ channel.

2. Material and methods

2.1. Molecular biology

The *Saccharomyces cerevisiae* open reading frame *TOK1*/*YJL093c*/*J0911* was isolated and cloned into pBluescriptII KS$^-$ (Stratagene, Heidelberg) as a 3.1 kb *Eco*RI-*Pst*I fragment derived from a 6.1 kb *Eco*RI-*Bgl*II clone (A1–A14 [12]). The plasmid was used for PCR amplification of the *TOK1* coding region. *Bal*I and *Stu*I restriction sites were introduced into the oligonucleotides immediately upstream of the ATG start and downstream of the TGA stop codons to replace the *Xenopus* β-globin coding region of the expression vector pBSXG1 [13]. The resulting pEXTM1 plasmid was linearised by digestion with *Hin*dIII and GppG-capped cRNA synthesized using T7 polymerase (Cap-Scribe kit, Boehringer).

2.2. Electrophysiology and analysis

Stage V and VI oocytes were taken from mature *Xenopus laevis* and maintained at 18°C in a modified Barth's medium containing 88 mM NaCl, 1 mM KCl, 0.33 mM $Ca(NO_3)_2$, 0.41 mM $CaCl_2$, 0.82 $MgSO_4$, 2.4 mM Na_2CO_3, 0.1 mg/ml gentamycin sulphate, and 80 U/ml penicillin. Oocytes were isolated mechanically after partial digestion of the follicular cell layer with 2 mg/ml collagenase (Sigma), and were injected with 1–30 ng cRNA in water following standard procedures [14]. Oocytes injected with water alone were used as controls.

Membrane current was recorded under voltage clamp in oocytes 2–5 days post injection using a two-electrode clamp circuit [15] under microprocessor control with a WyeScience μP amplifier and μLAB/μLAN analog/digital interface and software (WyeScience, Wye, UK). Measurements were carried out in a modified Ringer's solution containing 1 mM KCl, 99 mM NaCl, 1 mM $MgCl_2$ and buffered with 5 mM HEPES titrated to pH 7.5 with $Ca(OH)_2$ ($[Ca^{2+}] \simeq 1$ mM). Extracellular KCl was varied without altering the osmotic strength of the medium with an equivalent change in NaCl concentration or, in some experiments, by exchange with sorbitol against a background of 10 mM NaCl. No difference was observed between the two sets of data

*Corresponding author. Fax: (44) (1233) 813 140.
E-mail: mblatt@wye.ac.uk

PII S0014-5793(97)00211-1

(not shown), consistent with the insensitivity of the current to extracellular Na^+ (see text). Intracellular microelectrodes were bevelled manually and filled with 3 M KCl (input resistances, <0.1 MΩ). Connection to the amplifier headstage was via a 3 M KCl/Ag-AgCl halfcell, and a matching halfcell and 3 M KCl-agar bridge served as the reference (bath) electrode. The IR drop to ground was compensated by the voltage signal from a second electrode positioned in the bath. Current and voltage were nominally sampled at 1 or 2 kHz under voltage clamp and the current signal was filtered at 0.3 or 1 kHz prior to digitising. In some instances, steady-state current-voltage (I-V) relations were recorded using a bipolar staircase of command voltages and data recorded during the final 10 ms of each pulse [15].

Conductances were generally determined from joint fittings using a Marquardt-Levenberg algorithm [16]. Steady-state conductances were obtained from fittings to a Boltzmann function

$$I_K = \frac{g_{max}(V-E_K)}{1+e^{\delta F(V-V_{1/2})/RT}} \quad (1)$$

where I_K is the TOK1p current at voltage V, g_{max} is the maximum steady-state conductance, δ is the voltage-sensitivity coefficient (= apparent gating charge), $V_{1/2}$ is the voltage at which the steady-state conductance $g_s = g_{max}/2$, and F, R and T have their usual meanings. Because the current reversal potential could not be obtained directly from tail current analyses, the K^+ equilibrium voltage, E_K, was defined from the Nernst equation and fittings carried out jointly holding the parameter for the intracellular $[K^+]$ in common.

3. Results and discussion

3.1. Slowly activating component of TOK1p current is $[K^+]_o$-sensitive

Expression of *TOK1* was measurable within 24 h of cRNA injection and was characterised by large currents of 2–6 μA at 0 mV in the modified Ringer's medium (1 mM $[K^+]_o$). As reported previously [2,3], the TOK1p current rectified strongly outward and current relaxations could not be resolved in 1 mM $[K^+]_o$ at any voltage negative of E_K after positive voltage steps to activate the current; the chord conductance for the TOK1p current increased roughly in proportion with the logarithm of $[K^+]_o$ (Fig. 1b, inset) and the voltage yielding half-maximal activation of the current in the steady-state was displaced to more positive voltages as $[K^+]_o$ increased (see Fig. 1c, also Fig. 3c).

Two kinetic components contributed to TOK1p activation on membrane depolarisation. One component was sufficiently fast-activating as to be unresolved in these measurements. The second component activated slowly with roughly mono-exponential kinetics ($\tau \simeq 0.2$ s at 0 mV and in 1 mM $[K^+]_o$; see Fig. 1a). Lesage et al. [3] noted before that the current kinetics were biased to the slow-activating component by negative conditioning voltages, consistent with a serial transition of the channel between two closed states leading to a terminal open state and 'trapping' of the channel in the second (distal) closed state at negative voltages. We found, however, that total elimination of the fast-activating component was not possible in the presence of 1 mM $[K^+]_o$, and a significant fraction of the fast-activating component was present on positive voltage steps, even from a holding voltage of −100 mV (Fig. 1a, top) roughly 100 mV negative of the voltage yielding half-maximal conductance in 1 mM $[K^+]_o$ (Fig. 1c). By contrast, raising $[K^+]_o$ to 3 and 30 mM decreased this current component under the same voltage clamp conditions (Fig. 1a, centre and bottom). Because $[K^+]_o$ and (negative) membrane voltage otherwise affected the steady-state conductance similarly (Fig. 1c), these data suggested that the actions of $[K^+]_o$ and voltage on the two kinetic components might be distinct.

To characterise the voltage and $[K^+]_o$ sensitivities of the slow-activating component and distinguish these from the sum of slow- and fast-activating elements in the steady-state current, a two-step protocol was adopted (cf. Fig. 1a). Conditioning steps to voltages between −140 and +20 mV were used to establish different steady-state distributions of the channels between open and closed states. Currents recorded at the start of depolarising steps to voltages positive of −20 mV were used to determine the 'instantaneous' I-V curve and the corresponding instantaneous conductance, g_i, after correcting for background conductance determined at voltages negative of E_K. Fig. 2a shows that this instantaneous current approximated a linear function of clamp voltage over this voltage range. Thus, the effect of conditioning voltage on the current was separable from any effect of voltage on single-channel conductance, γ_K (see also [2,3]). At any one $[K^+]_o$, the effect of positive-going conditioning voltages was to increase g_i only, and the current and conductance could be related as $I = g_i(V-E_K)$.

Values of g_i for $[K^+]_o$ of 1, 3 and 30 mM are plotted as a function of the conditioning voltage in Fig. 2b after normalising to the maximal conductance at each $[K^+]_o$. The data were well-fitted by a Boltzmann function of the form

$$g_{rel} = \frac{1}{1+e^{\delta F(V-V_{1/2})/RT}} \quad (2)$$

where g_{rel} is relative conductance, δ is the voltage sensitivity coefficient (= apparent gating charge), $V_{1/2}$ is the voltage at which $g_{rel} = 0.5$, and F, R and T have their usual meanings. The most striking features of g_i were its component voltage and $[K^+]_o$ sensitivities. First, voltage had a diminished effect on g_i. For the curves shown, the limiting slope gave a e-fold rise in relative conductance for every +29 mV ($\delta \approx 0.84$) compared with an equivalent rise in conductance over +21 mV ($\delta \approx 1.26$) obtained for the steady state in the same experiment (Fig. 1). Furthermore, values for $V_{1/2}$ were situated well negative of the corresponding values for the steady-state current at any one $[K^+]_o$ (compare Fig. 1). Second, and by contrast, increasing $[K^+]_o$ displaced g_i to virtually the same extent as the steady-state conductance g_s (Fig. 1), in this case by +34 mV between 3 and 30 mM $[K^+]_o$. Because the two-step protocol effectively reported the fraction of the current associated with slow activation (see Section 3.4), these results suggested that the $[K^+]_o$ sensitivity of the TOK1p current was isolated kinetically to its slow-activating component while the voltage sensitivity of the current was distributed between both components.

Instantaneous and steady-state analyses, like those in Figs. 1 and 2, also appeared to yield a reduced $[K^+]_o$ sensitivity at concentrations near 1 mM, suggesting a site with moderate affinity for extracellular K^+ might confer $[K^+]_o$ sensitivity to the gating process. To test this possibility, measurements of steady-state conductance (g_s) were carried out while sequentially reducing $[K^+]_o$ below 1 mM. Instantaneous (g_i) conductances were also assayed since, for the serial gating process (see Section 3.4), both were expected to show parallel, and limited sensitivity to $[K^+]_o$. Table 1 summarises values for $V_{1/2}$ determined for g_s and corresponding values of g_i taken at a common, representative voltage, but over the range of 0.01–1 mM $[K^+]_o$ from 6 independent experiments. As anticipated, reducing $[K^+]_o$ to concentrations below 1 mM had little influence on either parameter, again consistent with a direct

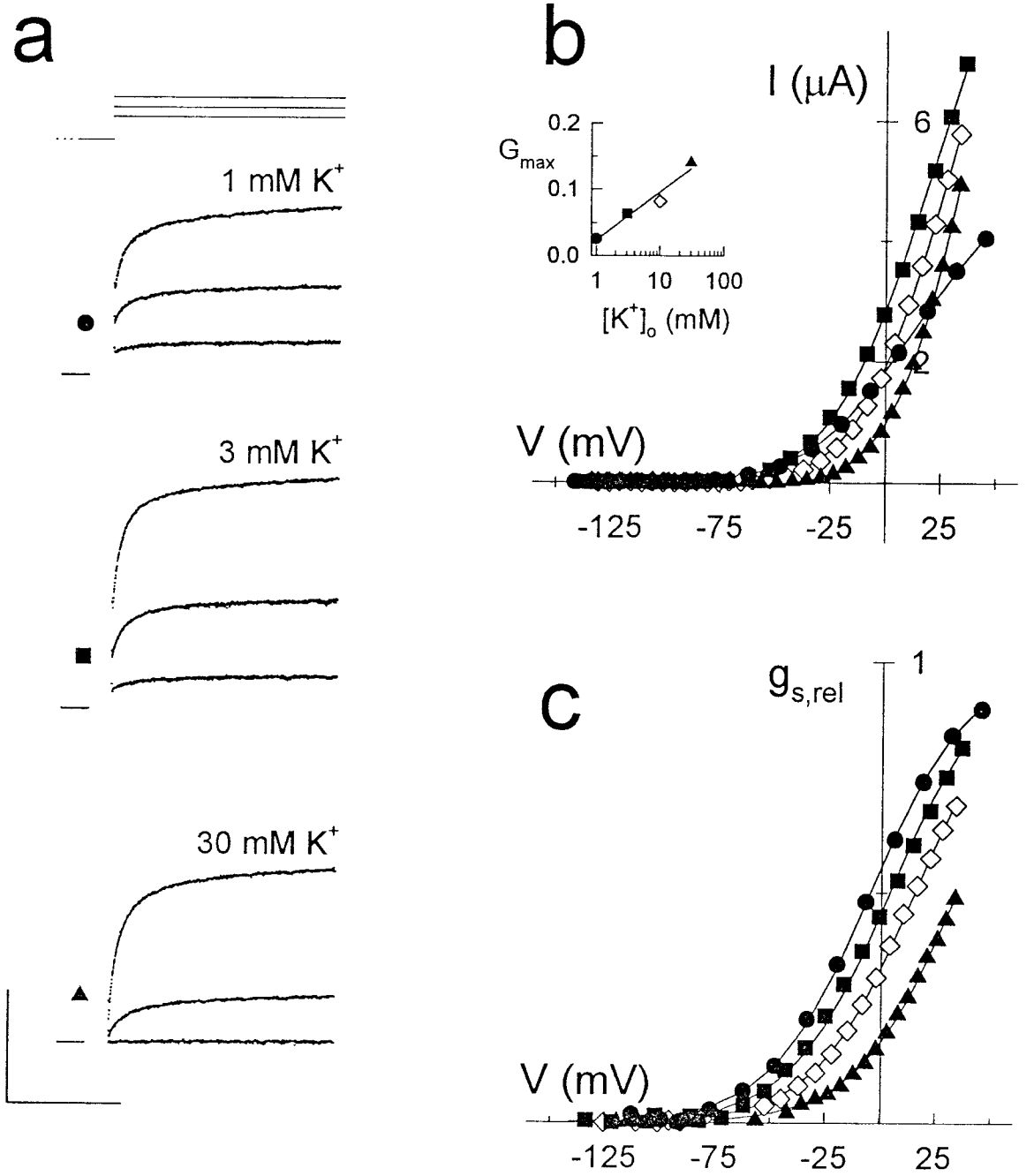

Fig. 1. Extracellular $[K^+]$ affects the voltage sensitivity of steady-state TOK1p current and the relative contributions of its fast- and slow-activating components. Data from one oocyte bathed in Ringer solutions after subtracting background currents determined by linear extrapolation of steady-state currents measured between −160 and −140 mV. (a) Current trajectories recorded at −30, 0 and +30 mV in 1 mM (●, top), 3 mM (■, centre) and 30 mM $[K^+]_o$ (▲, below) following 10-s conditioning steps to −100 mV (top). Current zero indicated on left. Scale: 300 mV or 2 μA (vertical), 2 s (horizontal). (b) Steady-state current-voltage curves recorded using a bipolar staircase protocol. Data are for 1 mM (●), 3 mM (■), 10 mM (☆) and 30 mM $[K^+]_o$ (▲) and were fitted jointly (solid lines) to Eq. 1. Inset: Maximum steady-state conductance, $g_{s,max}$, as a function of the logarithm of $[K^+]_o$. Symbols cross-referenced to b and c. (c) Normalised steady-state conductances derived from the fittings in b. Fitted parameters: $g_{s,max}$, 0.26 mS [1], 0.64 mS [3], 0.82 mS [10], 1.40 mS (30 mM $[K^+]_o$); $V_{1/2}$, −5 mV [1], +5 mV [3], +16 mV [10], +36 mV (30 mM $[K^+]_o$); δ (common), 1.16; $[K^+]_i$ (common), 127 mM.

transfer of the action of $[K^+]_o$ on the slow component to gating of the TOK1p current in the steady state.

3.2. Block of TOK1p current by Ba^{2+} is voltage-dependent

The crystal radius of Ba^{2+} is very close to that of K^+, making the divalent an efficient K^+ channel blocker at low millimolar concentrations in many cells [7,17,18]. Yeast K^+ channels [19,20] have been reported to be sensitive to Ba^{2+}, but for TOK1p the divalent has been mooted [3] to be roughly 150-fold more effective in blocking the fast-activating component of the current (K_i, 20 μM compared with 3 mM for the slow-activating component; see also [11]), implicating two cation binding sites within the TOK1p pore. The same dependence on $[Ba^{2+}]$ might be understood, however, if Ba^{2+}

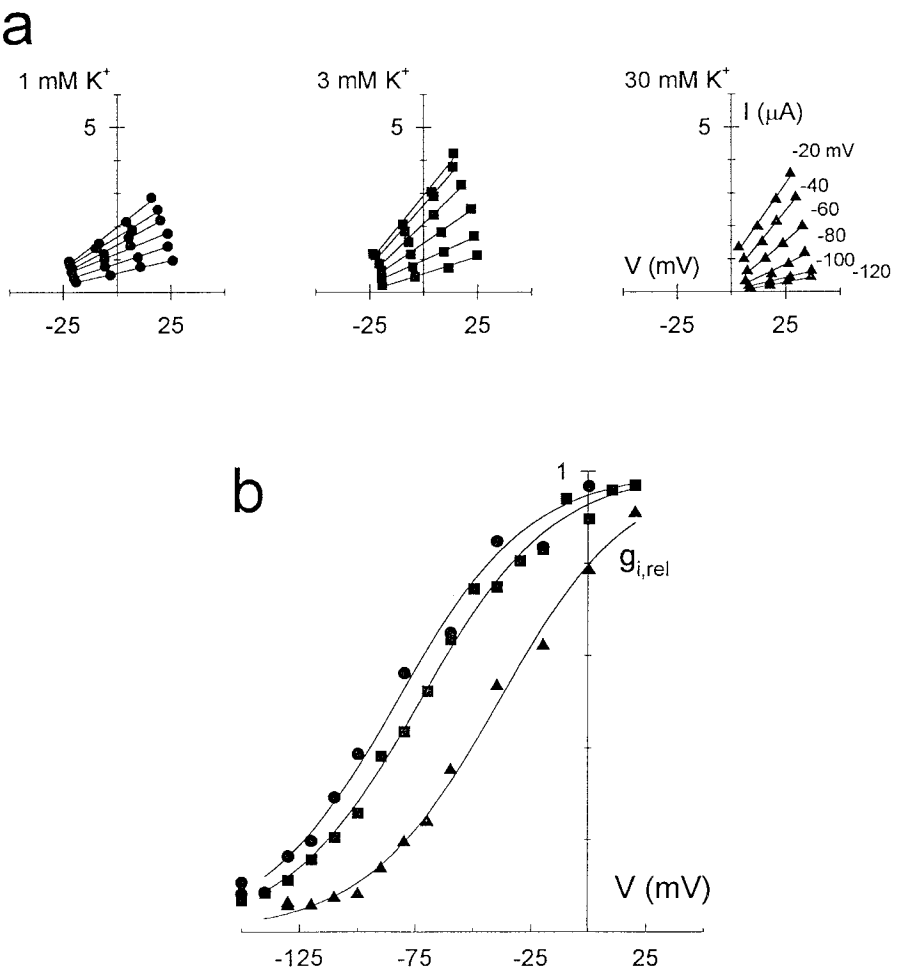

Fig. 2. Action of $[K^+]_o$ on TOK1p current is accommodated by the $[K^+]_o$ sensitivity of the slow-activating component. Data from the same oocyte as in Fig. 1. (a) Instantaneous TOK1p currents recorded during 2-pulse protocols (see Fig. 1). Data points taken 4 ms into test voltage clamp steps between −25 and +40 mV from conditioning voltage steps (10 s) at voltages indicated (right, −120 to −20 mV) after subtracting background currents (see Fig. 1). Measurements taken in 1 mM (left), 3 mM (centre) and 30 mM $[K^+]_o$ (right). (b) Relative instantaneous conductance, $g_{i,rel}$ ($=g_i/g_{i,max}$) determined from joint fitting to Eq. 2. Fitted parameters: $V_{1/2}$, −83 mV [1], −74 mV [3], −38 mV (30 mM $[K^+]_o$); δ (common), 0.87.

– like K^+ – affected the voltage dependence of the gating process, and this possibility prompted us to reinvestigate block of the current by Ba^{2+}.

Fig. 3a shows the results of voltage clamp measurements at +30 mV in 1 mM $[K^+]_o$ after conditioning with voltages of −100 mV, −50 and 0 mV first in the absence, and then in the presence of 0.1 and 1 mM Ba^{2+}. Relative steady-state and instantaneous conductances are summarised in Fig. 3b,c. Equivalent results were obtained in three further, independent experiments. Increasing external $[Ba^{2+}]$ reduced the magnitude of the fast-activating component of TOK1p current recorded following a given conditioning voltage, but the effect could be fully compensated when clamp steps were preceded by more positive conditioning voltages (Fig. 3a). In other words, extracellular Ba^{2+} displaced the apparent voltage sensitivity of the TOK1p current to increasingly positive voltages like $[K^+]_o$. The effect was to shift $V_{1/2}$ by +19 mV/$[Ba^{2+}]$ decade between 100 μM and 1 mM Ba^{2+}, roughly equivalent to the effect of $[K^+]_o$ at concentrations 10-fold higher. Also like K^+, Ba^{2+} action was mediated through the slow-activating component of the current, as indicated by the equivalent shifts in the $g_{i,rel}$-V and $g_{s,rel}$-V curves (Fig. 4c). However, Ba^{2+} additions also increased the limiting voltage sensitivities of these parameters: for the data shown, δ values for g_s increased from 1.39 to 1.68 and for g_i rose from 0.71 to 1.38 in the absence and presence of 1 mM Ba^{2+}, respectively. Adding Ba^{2+} also increased the steady-state current magnitude at voltages near 0 mV (Fig. 4a, below), indicating that its interaction with the channel could not be understood simply in terms of an occlusion of the pore and 'knock-out' by K^+ efflux at positive voltages.

Table 1
$[K^+]_o$ sensitivity of TOK1p gating is lost at $[K^+]_o$ below 1 mM

$[K^+]_o$/mM	0.01	0.1	1
$V_{1/2}$/mV	−7 ±2	−9 ±1	−8 ±2
g_i (rel)	0.22 ± 0.02	0.23 ± 0.03	0.26 ± 0.03

Values of $V_{1/2}$ determined as in Fig. 1 by joint fittings of steady-state TOK1p currents to Eq. 1. Joint parameters: δ, 1.35 ± 0.05; a_K, 115 ± 8 mM. Relative instantaneous conductance, g_i, determined from voltage steps to potentials between −20 and +30 mV following conditioning steps at −120 mV. Values are means ± S.E. of 6 independent measurements.

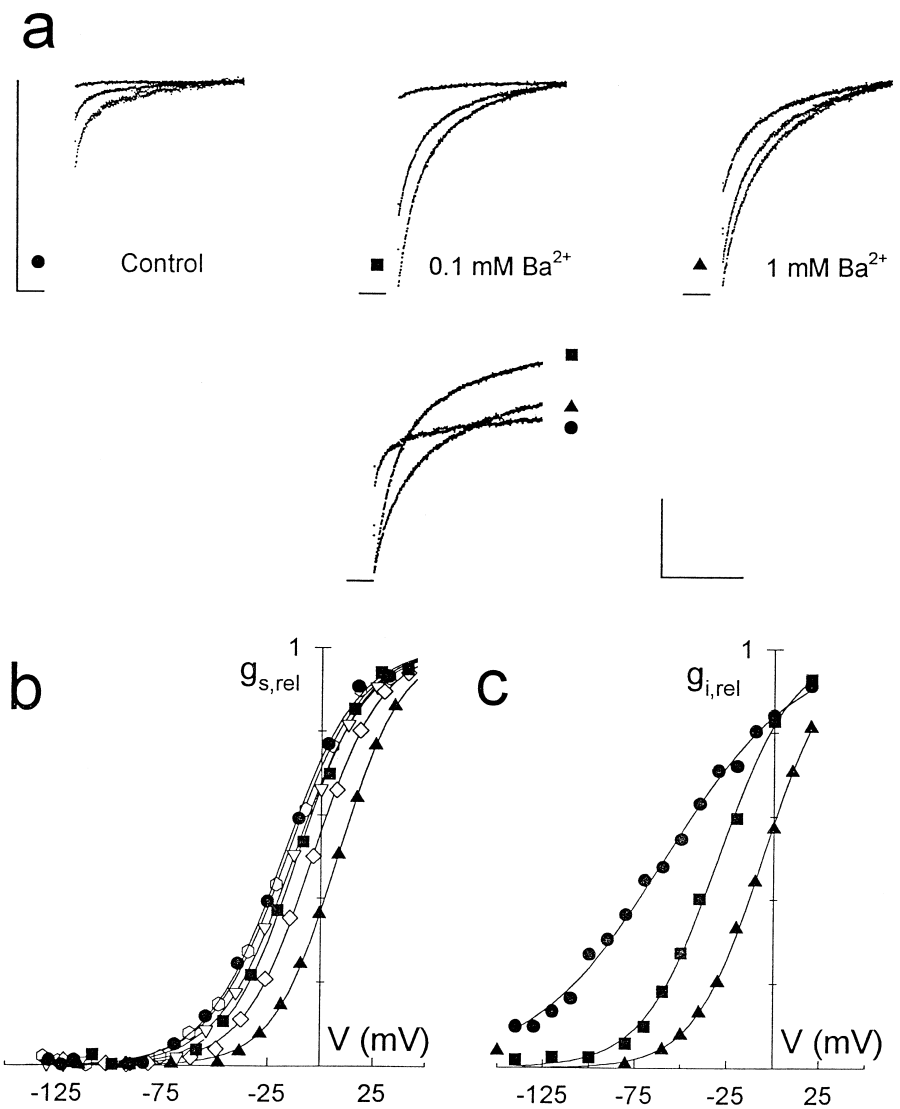

Fig. 3. Micromolar extracellular Ba^{2+} effects a voltage-dependent 'block' of the TOK1p current, but promotes its maximum conductance and steady-state current at positive voltages. Data from one oocyte bathed in 1 mM KCl Ringer after subtracting background current (see Fig. 1). (a) TOK1p current trajectories normalised to the current maxima (vertical bar, left) in the absence (●, left) and presence of 0.1 mM (■, centre) and 1.0 mM Ba^{2+} outside (▲, right). All test voltage steps at +30 mV and preceded by 10-s conditioning steps to −100, −50 and 0 mV (lowermost, centre, and uppermost in each set of three trajectories). Zero current levels indicated and measurements cross-referenced by symbol to b and c. (Below) Raw TOK1p currents recorded following conditioning steps at −100 mV, but without normalisation. Scale: 1 μA (vertical), 1 s (horizontal). (b) Relative steady-state conductance, $g_{s,rel}$, determined as in Fig. 1. Additional symbols correspond to data gathered in 10 μM (hexagon), 30 μM (▽) and 300 μM Ba^{2+} (◇). Fitted parameters: $g_{s,max}$, 0.52 mS (control), 0.60 mS (10 μM), 0.62 mS (30 μM), 0.63 mS (100 μM), 0.74 mS (300 μM), 1.00 mS (1 mM $[Ba^{2+}]_o$); $V_{1/2}$, −19 mV (control), −17 mV (10 μM), −14 mV (30 μM), −11 mV (100 μM), −4 mV (300 μM), +8 mV (1 mM $[Ba^{2+}]_o$); δ, 1.41 (control), 1.43 (10 μM), 1.43 (30 μM), 1.54 (100 μM), 1.56 (300 μM), 1.68 (1 mM $[Ba^{2+}]_o$). (c) Relative instantaneous conductance, $g_{i,rel}$, determined as in Fig. 2. Fitted parameters: $V_{1/2}$, −59 mV (control), −30 mV (100 μM), −4 mV (1 mM $[Ba^{2+}]_o$); δ, 0.71 (control), 1.26 (100 μM), 1.38 (1 mM $[Ba^{2+}]_o$).

3.3. *Cation- and voltage-sensitivities implicate a common action on gating*

To assess the specificity of Ba^{2+} and K^+ action on the TOK1p current, additional experiments were carried out exchanging K^+ with Rb^+ and Cs^+, raising $[Ca^{2+}]_o$ and $[Mg^{2+}]_o$, and reducing $[Na^+]_o$. Adding 10 mM Ca^{2+} or Mg^{2+} had no measurable effect on the voltage sensitivity of the current (not shown), nor did a 10-fold change in $[Na^+]_o$. However, Rb^+ was as effective as or more effective than K^+ in displacing the TOK1p current characteristic along the voltage axis, and even the K^+ channel blocker Cs^+ was able to substitute for K^+ (Table 2). These results demonstrated a specificity among cations[1] and, furthermore, highlighted a parallel to the relative ionic selectivities of many K^+ channels [1]. From the relative efficacies in displacing $V_{1/2}$, TOK1p gating was consistent with the Eisenman II series for alkali cations (efficacy $Rb^+ > Cs^+ > K^+ > Na^+$ [21]). Together with evidence for the finite sensitivity to extracellular K^+ and Ba^{2+} concentrations, these observations suggest a ligand-controlled gate with

[1] The observations also discount an action on the gating process mediated by screening of bulk surface charge [1] or a direct interaction of extracellular Ca^{2+} with the TOK1p channel. A role for Ca^{2+} in TOK1p gating was proposed initially [2], but could not be confirmed in subsequent Ca^{2+}-depletion studies [3].

an ion binding site of weak field strength and an affinity for alkali cations in the low millimolar range. Furthermore, they implicate a gate that *in*activates or blocks the channel upon cation binding, whether of Ba^{2+} or K^+.

In order to quantify the nature and efficacy of extracellular K^+ action, the currents in Figs. 1 and 2 and additional data sets were plotted as a functions of K^+ 'block' relative to TOK1p currents recorded in 1 mM $[K^+]_o$. As shown in Fig. 4a, the transformation yields families of isopotential values that approximate simple hyperbolic binding characteristics. Jointly, the data were well-fitted to the Hill equation with an apparent cooperativity coefficient n of 1 (mean ± S.E., 1.1 ± 0.1), consistent with the binding of a single K^+ ion to effect block of the TOK1p current. The analysis also showed that increasing (positive-going) clamp voltages effected a decrease in the apparent affinity for external K^+ (increasing K_d). This characteristic, summarised in Fig. 4b, indicated a limiting voltage sensitivity (solid line) equivalent to an e-fold increase in the affinity for K^+ per −26 mV change in membrane voltage. Similar analysis of Ba^{2+} action on the TOK1p current yielded an equivalent absence of cooperativity (n=0.97 ± 0.03), but higher apparent affinity and a limiting voltage dependence equivalent to an e-fold rise in affinity per -14 mV (Fig. 4b, dotted line), or roughly twice that of K^+, as expected for a cation with a valency of +2.

3.4. A model for TOK1p gating by extracellular K^+

The simplest kinetic model consistent with the voltage dependence of the TOK1p current comprises two closed states of the channel that communicate with each other, and a terminal open state

$$C_3 \underset{k_{32}}{\overset{k_{23}}{\leftrightharpoons}} C_2 \underset{k_{21}}{\overset{k_{12}}{\leftrightharpoons}} O_1 \qquad (3)$$

with corresponding reaction constants, as shown. With the reaction constants k_{21} and k_{12} very large relative to k_{32} ($C_2 \leftrightharpoons O_1$ fast relative to $C_3 \leftrightharpoons C_2$) and both transitions sensitive to membrane voltage, this interpretation accounts for observations (Figs. 1 and 2) of two distinct kinetic components to the current relaxations on depolarising voltage steps, the effect of conditioning voltage on the relative distribution between the fast- and slow-activating components, and the absence of appreciable tail currents on membrane hyperpolarisation. These characteristics were exploited in two-pulse protocols to separate the voltage and $[K^+]_o$ dependencies of the two kinetic components. The fast transition – and hence contributions to the instantaneous current from channels in state C_2 and O_1 at the end of conditioning voltages – could not be resolved. Therefore, $g_{i,rel}$ effectively reflects the relative occupancy of the distal closed state C_3 and the rate constants k_{32} and k_{23} which, in turn, determine the slow-activating component of the current. Equally, K^+ binding may be isolated to the $C_3 \leftrightharpoons C_2$ state transition, since the effect of $[K^+]_o$ on $g_{i,rel}$ and the slow-activating component proved sufficient to account for the $[K^+]_o$ sensitivity of the TOK1p conductance as a whole (Figs. 1 and 2). By contrast, the voltage sensitivity of the gate was distributed between the $C_3 \leftrightharpoons C_2$ and $C_2 \leftrightharpoons O_1$ transitions, as indicated by the lower values of δ and the displacement of values for $V_{1/2}$ to more negative voltage for g_i compared with g_s (Figs. 2 and 3).

Features of $[K^+]_o$ action on the TOK1p channel and their parallel with block of the current by Ba^{2+} also suggest a physical model for gating. The complementary sensitivities to voltage, ionic concentration and species are consistent with specific binding of external K^+ and Ba^{2+} at a single site (or equivalent sites) well-within the membrane electric

Table 2
Rb^+ and Cs^+ substitute for K^+ in modulating the voltage sensitivity of TOK1p gating

	1 mM	10 mM $[K^+]_o$	10 mM $[Rb^+]_o$	10 mM $[Cs^+]_o$
$V_{1/2}$/mV	−11 ± 2	+12 ± 3	+14 ± 2	+23 ± 2

Values of $V_{1/2}$ from measurements in 1 and 10 mM $[K^+]_o$, and after substituting with 10 mM $[Cs^+]_o$ and 10 mM $[Rb^+]_o$. Parameters determined as in Fig. 1 assuming $P_x = P_K$. Assigning values consistent with 10:1 selectivities ($P_x = P_K/10$) gave similar results, but with $V_{1/2}$ displaced an additional +14 mV relative to that for 10 mM $[K^+]_o$. Values are means ± S.E. of (n) independent measurements.

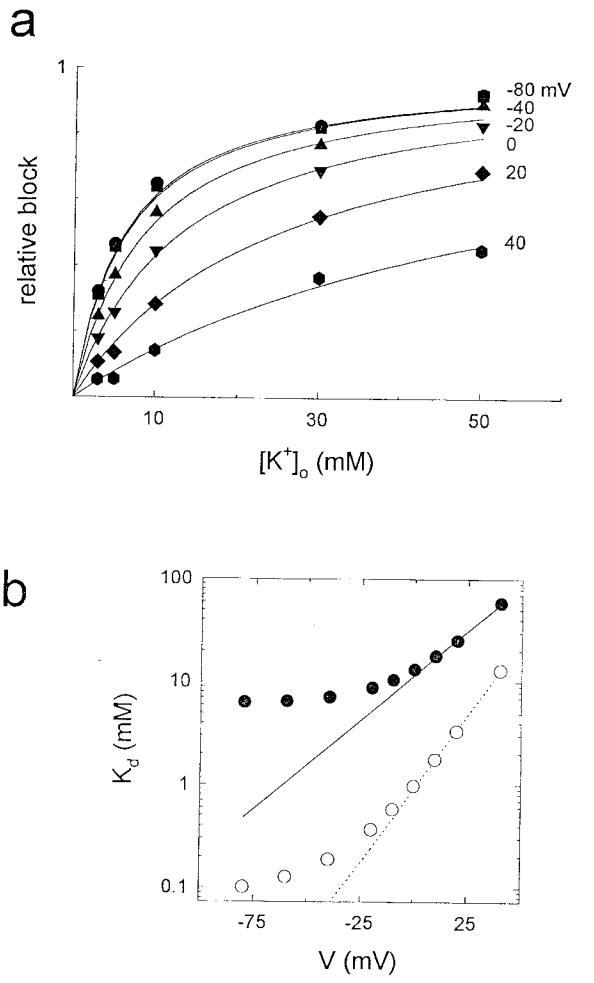

Fig. 4. Isopotential transformation of relative steady-state conductances indicate a mass-action effect of extracellular K^+ and Ba^{2+} leading to complete inactivation of TOK1p current. (a) Transformations of $g_{s,rel}$, including data in Fig. 1, to give apparent relative block ($=1-g_{s,rel}$) at voltages between −80 and +40 mV (right) and fitted jointly to the Hill equation with the Hill coefficient constrained to 1.0. (b) Apparent binding constants for K^+ (●) derived from a and plotted against clamp voltage. Also shown are results of similar analyses for Ba^{2+} (○, see Fig. 3). Limiting voltage sensitivities indicated by the solid (K^+) and dotted (Ba^{2+}) lines determined by regression analysis of points at +10, +20 and +40 mV. Apparent voltage sensitivity coefficient: 0.94 (K^+), 1.84 (Ba^{2+}).

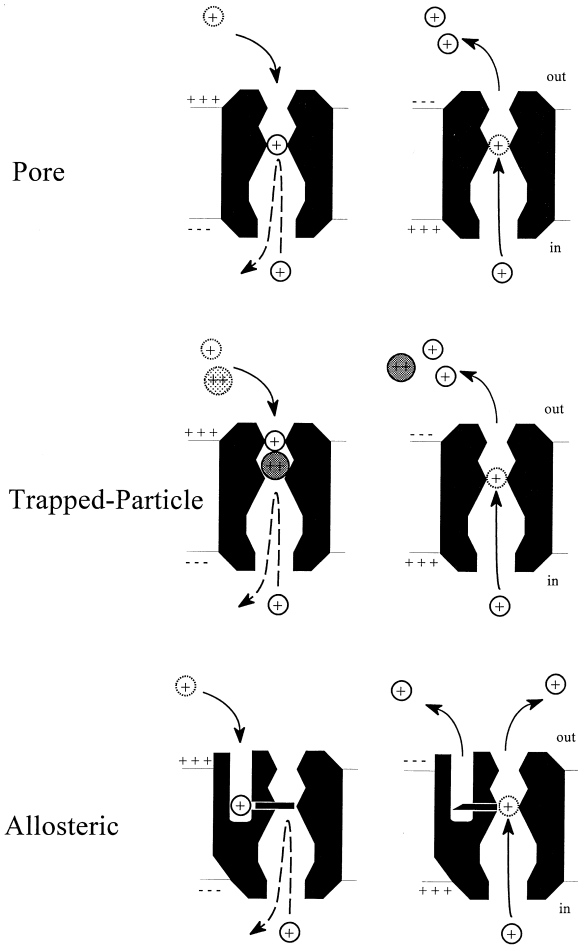

Fig. 5. Physical models for K^+ channel gating. All three models comprise binding sites within the pore that are accessible to K^+ ions from both sides of the membrane. Origins and movement of blocking or gating particles are shown by the dotted particle symbols. Singly charged species indicate the nominally permeant ionic species. The pore model identifies access from outside with block or closure of the pore and access from inside with ion permeation. The trapped-particle model postulates that entry of a non-permeant blocking particle – as shown from free solution and carrying a double charge, or as particle tethered to the channel outside [2,3] – results in block or closure when the particle becomes trapped within the pore by a permeant ion entering from behind. The allosteric model proposes a binding site, within the membrane electric field but distinct from the pore, that shuts the gate when occupied.

field to give an inactivation of the TOK1p current through a simple mass action effect (Fig. 4). Both K^+ and Ba^{2+} displaced the apparent voltage sensitivity of the TOK1p current to increasingly positive voltages, and the actions of both cations on the current were accommodated by the slow-activating component (Figs. 2 and 3). The limiting voltage sensitivity evident in the apparent K_d for Ba^{2+} action was roughly twice that for K^+ (Fig. 4). Furthermore, Ba^{2+} additions resulted in progressive and parallel increases in δ for both g_i and g_s. These latter observations, especially, are consistent with competition between Ba^{2+} and K^+ for binding to a single site.

Three possible physical interpretations for K^+ binding and control of TOK1p are shown in Fig. 5. In the first case (pore model), K^+ or 'K^+-like' ions are proposed to enter the pore from outside and to bind at a site within the permeation pathway effecting a block or closing of a 'K^+ gate'. Increasing concentrations of these ions outside necessitate a corresponding increase in opposing electrical field strength to displace the blocking ion and open the channel. This hypothesis is equivalent to 'gating particle' models [1,22] in which the charge displacement of K^+ or a 'K^+-like' ion to the binding site(s) confers voltage dependence to the process. The trapped-particle model is a variant of the pore model and postulates an unique ('non-K^+') charged blocking particle that, once in the pore, becomes trapped by K^+ entering from outside [2,3]. The third model (allosteric model) postulates an external cation binding site within the membrane electric field, but distinct from the permeation pathway, that controls the 'K^+ gate' of the channel.

An attractive feature of the pore model lies in the close correspondence between the gating charge for TOK1p of approximately 1 (Fig. 1), the apparent requirement for binding of one K^+ in gating and voltage-sensitivity for K^+ binding (Fig. 4). The affinity for K^+ showed an e-fold rise per −26 mV which, with a single K^+ ion binding at a site after traversing virtually the full electrical distance across the membrane, would account for the bulk of voltage sensitivity of the TOK1p conductance. This argument aside, we favour the allosteric model because, unlike the pore model and variants, it identifies external cation access for gating and for permeation unambiguously. A major difficulty with the pore model lies in separating the actions of K^+ (or another cation) entering from outside and from the inside without violating physical laws of microscopic reversibility. For gating of TOK1p, it suggests that access of K^+ ions from outside to sites in the pore effects a block of the channel, yet access of K^+ from the inside to the same sites contributes to ion permeation! By contrast, the allosteric model separates $[K^+]_o$-sensitivity and K^+ permeation, and it can accommodate two binding sites with differing affinities for Ba^{2+}, one at the regulatory site and the second in the channel pore. The effect of external K^+ (and at low concentrations, Ba^{2+}) binding in this case might be to alter charge/dipole moments of the gate or their environment through protein conformational changes [23,24]. The trapped-particle model cannot be wholly excluded at present. However, the additional charge accompanying such a particle and the K^+ ion outside would not accord so readily with the unitary gating charge (Fig. 1) or Hill coefficient for K^+ inactivation (Fig. 4). Trapping of external Ca^{2+} [2] seems even less likely for this reason, quite apart from the lack of any appreciable effect of $[Ca^{2+}]_o$.

4. Conclusion

The yeast K^+ channel encoded by the *TOK1* gene shows structural and physiological features unique among outward-rectifying K^+ channels cloned so far. Gating characteristics of TOK1p are allied to those of outward-rectifying K^+ channels from higher plants in which extracellular K^+ and membrane voltage coordinately regulate ensemble channel conductance [8,9]. Analysis of TOK1p gating demonstrates a cation selectivity predicted by the Eisenman II series [21] and indicates voltage and $[K^+]_o$ sensitivities in accord with a single gating charge and the binding of one K^+ ion to effect closure of the gate. Additional evidence, including a dual action of Ba^{2+} at submillimolar concentrations as K^+-mimetic for gating and at millimolar concentrations as a channel blocker, implicate that

cation binding associated with the gate occurs at a site outside the pathway for ion permeation through the channel pore.

Acknowledgements: We are grateful to G. Thiel (Göttingen) and A. Bertl (Karlsruhe) for comments on the manuscript. This work was made possible in part by grants-in-aid from the Gatsby Charitable Foundation (M.R.B.) and the Deutsche Forschungsgemeinschaft (T.M.). P.V. is funded by the British Biotechnology and Biological Sciences Research Council (Grant 32/C04145).

References

[1] Hille, B. (1992) Ionic Channels of Excitable Membranes, Sinauer Press, Sunderland, MA.
[2] Ketchum, K.A., Joiner, W.J., Sellers, A.J., Kaczmarek, L.K. and Goldstein, S.A.N. (1995) Nature 376, 690–695.
[3] Lesage, F., Guillemare, E., Fink, M., Duprat, F., Lazdunski, M., Romey, G. and Barhanin, J. (1996) J. Biol. Chem. 271, 4183–4187.
[4] Jan, L.Y. and Jan, Y.N. (1994) Nature 371, 119–122.
[5] Catterall, W.A. (1995) Annu. Rev. Biochem. 64, 493–531.
[6] MacKinnon, R. (1995) Neuron 14, 889–892.
[7] Tester, M. (1990) New Phytol. 114, 305–340.
[8] Blatt, M.R. (1991) J. Membr. Biol. 124, 95–112.
[9] Blatt, M.R. and Thiel, G. (1993) Annu. Rev. Plant Physiol. Mol. Biol. 44, 543–567.
[10] Zhou, X.L., Vaillant, B., Loukin, S.H., Kung, C. and Saimi, Y. (1995) FEBS Lett. 373, 170–176.
[11] Reid, J.D., Lukas, W., Shafaatian, R., Bertl, A., Scheurmann-kettner, C., Guy, H.R. and North, R.A. (1996) Receptors Channels 4, 51–62.
[12] Miosga, T., Witzel, A. and Zimmermann, F.K. (1994) Yeast 10, 965–973.
[13] Groves, J.D. and Tanner, M.J.A. (1992) J. Biol. Chem. 267, 22163–22170.
[14] Gould, G.W. (1994) Membrane Protein Expression Systems, Portland Press, London.
[15] Blatt, M.R. (1987) J. Membr. Biol. 98, 257–274.
[16] Press, W., Flannerly, B., Teukolsky, S. and Vetterling, W. (1986) Numerical Recipes: The Art of Scientific Computing, Cambridge University Press, Cambridge.
[17] Slesinger, P.A., Jan, Y.N. and Jan, L.Y. (1993) Neuron 11, 739–749.
[18] Miller, C., Latorre, R. and Reisin, I. (1987) J. Gen. Physiol. 90, 427–449.
[19] Gomez, L.F., Pena, A., Lievano, A. and Darszon, A. (1989) Biophys. J. 56, 115–120.
[20] Sato, M., Tanifuji, M. and Kasai, M. (1989) Cell Struct. Funct. 14, 659–668.
[21] Eisenman, G. and Horn, R. (1983) J. Membr. Biol. 76, 197–225.
[22] Frankenhaeuser, B. and Hodgkin, L. (1957) J. Physiol. 137, 218–244.
[23] Neyton, J. and Pelleschi, M. (1991) J. Gen. Physiol. 97, 641–665.
[24] Armstrong, C.M. and Matteson, D.R. (1986) J. Gen. Physiol. 87, 817–832.